Biophysical Chemistry 137 (2008) 24–27

Contents lists available at ScienceDirect

Biophysical Chemistry

journal homepage: http://www.elsevier.com/locate/biophyschem

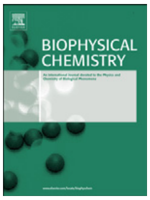

Correlation between Raman and X-ray crystallography data of $(Pro\text{-}Pro\text{-}Gly)_{10}$

Antonello Merlino [a], Filomena Sica [a,b,c], Lelio Mazzarella [a,b,c], Adriana Zagari [b,d,e], Alessandro Vergara [a,b,c,*]

[a] *Dipartimento di Chimica, Università degli Studi di Napoli "Federico II", Complesso Monte S. Angelo, Via Cinthia, I-80126. Naples, Italy*
[b] *Istituto di Biostrutture e Bioimmagini, CNR, via Mezzocannone 16, I-80134 Naples, Italy*
[c] *Consorzio Bioteknet, University of Naples, Italy*
[d] *Dipartimento delle Scienze Biologiche and CNISM, Università degli Studi di Napoli "Federico II", Via Mezzocannone 16, I-80134 Naples, Italy*
[e] *CEINGE-Biotecnologie Avanzate, Scarl, Naples, Italy*

ARTICLE INFO

Article history:
Received 22 May 2008
Received in revised form 16 June 2008
Accepted 16 June 2008
Available online 21 June 2008

Keywords:
Raman crystallography
Collagen
Amide bands
Proline puckering

ABSTRACT

Model biopolymers are powerful tools to guide the interpretation of physical properties in complex systems. $(Pro\text{-}Pro\text{-}Gly)_{10}$, $(PPG)_{10}$, is a collagen-model peptide, whose structure is known at high resolution. Herein, Raman microscopy data of $(PPG)_{10}$ powders and single crystals are reported. The spectra interpretation leads to an accurate assignment of three well-resolved amide bands corresponding to the three peptide bonds (PP, PG and GP) present in the $(PPG)_{10}$ structure. These data together with the availability of torsional angles φ and ψ derived from the high-resolution crystal structure, provide the opportunity to test the validity of theoretical equations for the calculation of non-canonical amide III bands and represent a reference for theoretical calculations of vibrational spectra and for polyproline II detection in complex proteins. Spectroscopic data do not support the indication of two distinct and equally populated *up* and *down* conformations of the pyrrolidine rings observed in the $(PPG)_{10}$ crystal structure.

1. Introduction

Collagen, the most abundant protein in animals, readily forms fibers, which yield mechanical support to skin, tendons and bones. In the last decade, a variety of collage-model polypeptides have been synthesized and characterized, and they have shed light on peculiar features related to collagen structure and stability.

Two of these collagen models, $(Pro\text{-}Pro\text{-}Gly)_{10}$, referred to as $(PPG)_{10}$, and $(Pro\text{-}Hyp\text{-}Gly)_{10}$ (POG) adopt a structural motif typical of a triple helix. $(PPG)_{10}$ is well characterized both from a structural [1] and a thermodynamic [2] point of view. Particularly, the melting temperature associated to the trimer disassembly is around 40 °C [2]. The low-resolution picture of $(PPG)_{10}$ shows a cylinder with length and diameter of 8.6 and 1.5 nm, respectively. The high-resolution (1.3 Å) crystallographic structure of $(PPG)_{10}$ (Protein Data Bank code 1 K6F) revealed accurate φ and ψ angles, and an alignment between chains driven by the charged extremity (N and C terminals) [1]. Based on high-resolution structural information of $(PPG)_{10}$ [1], generalized as $(X\text{-}Y\text{-}G)_{10}$, a new hypothesis was proposed for the extra stabilization induced by Hyp in Y [3]. This hypothesis is based on intrinsic conformational propensities of pyrrolidine rings within the triple helix of $(X\text{-}Y\text{-}Gly)_{10}$. According to this hypothesis, proline rings in the X position take *down* puckering and those in the Y position take *up* puckerings. Here, *up* and *down* puckerings correspond to the negative and positive values of χ_1 dihedral angles, respectively. This strict dependence of proline puckering on its position in the triplet was first observed at 100 K inside the $(PPG)_{10}$ crystals for the inner proline residues [1], though the equivalent structure for $(PPG)_9$ revealed that five proline residues at the Y position are in a *down* puckering conformation [4]. Furthermore, NMR study of $(POG)_{10}$ in an aqueous solution showed that proline residues at the X position have a *down* puckering conformation [5]. Successively, proline ring puckering of $(Pro\text{-}Hyp\text{-}Gly)_{10}$ was re-examined using X-ray diffraction data collected at high resolution (1.26 Å) in order to obtain reliable information both at 100 K and room temperature [6]. At 100 K, all the seven Hyp residues in the asymmetric unit at the Y position show *up* puckerings, while proline rings at the X position take three *up* and four *down* puckerings. Differently, at room temperature, X position has one *up* and six *down* puckerings in $(Pro\text{-}Hyp\text{-}Gly)_{11}$. The crystal structure of $(GOO)_9$ shows even *up* puckering of the proline ring in the X position [7].

Raman spectroscopy has been extensively used on protein systems in order to investigate secondary structure features [8], ligand binding [9], Se-Met incorporation [10], disulfide-bridge formation and conformation [11]. Raman microscopy is a valuable tool in assisting biocrystallographers [12,13], and it is now available on synchrotron beamlines [14]. Many Raman studies have been conducted to detect polyproline II conformation in oligo- [15,16], polypeptides and proteins [17]. Raman optical activity [18] and UV-Raman resonance spectroscopy [19] are also valuable tools to extract secondary structural details. *Ab initio* studies [20] and semi-empirical

---

* Corresponding author. Dipartimento di Chimica, Università degli Studi di Napoli "Federico II", Complesso Monte S. Angelo, Via Cinthia, I-80126. Naples, Italy. Tel.: +39 081 674259; fax: +39 081 674090.
E-mail address: avergara@unina.it (A. Vergara).

0301-4622/$ – see front matter © 2008 Elsevier B.V. All rights reserved.
doi:10.1016/j.bpc.2008.06.008

relationships [21,22] of amide I and III bands (IR inactive) with torsional angles φ and ψ are also available. The availability of polypeptides such as $(PPG)_{10}$ with a repetitive primary structure [only three types of peptide bonds (PP, PG and GP)], and a unique polyproline II secondary structure in a pure triple-helix quaternary structure provides the opportunity to define a relationship between vibrational properties and high-resolution structural details.

2. Materials and methods

2.1. Materials

$(PPG)_{10}$ powders were purchased from Peninsula Laboratories. The other chemicals used in this work were purchased from Sigma Chemical Co.

2.2. $(PPG)_{10}$ crystallization

Granada crystallization boxes [23] have been used to crystallize $(PPG)_{10}$. $(PPG)_{10}$ crystals have been grown as reported in Ref. [1] and have an average size of $0.2 \times 0.2 \times 0.1$ mm^3.

2.3. Raman microscopy

A confocal Raman microscope (Jasco, NRS-3100) was used to obtain Raman spectra of $(PPG)_{10}$ powders and single crystals. The 632.8-nm line of a He–Ne laser (1 mW at the sample), was injected into an integrated Olympus microscope and focused to a spot size of approximately 4 µm by a 20× objective. A holographic notch filter was used to reject the excitation laser line. The Raman backscattering was collected at 180°, using a 0.1-mm slit and a diffraction lattice of 1200 groove/mm corresponding to an average spectral resolution of 4 cm^{-1}. It takes 200 s both for crystals and powders to collect a complete data set by a Peltier-cooled 1024×128 pixel CCD photon detector (Andor DU401BVI). Wavelength calibration has been performed by using polystyrene as a standard. Raman microscopy measurements on $(PPG)_{10}$ samples were conducted transferring crystals into a hanging drop reactor using the same setup described in Ref. [10].

3. Results and discussion

A Raman microscopy study was conducted on $(PPG)_{10}$ powders and single crystals. $(PPG)_{10}$ crystals grown for this Raman studies are isomorphous with those used for the structural determination [1]. Spectra at low (400–1200 cm^{-1}) and high (1200–1700 cm^{-1}) frequencies are reported in Fig. 1A and B. The Raman spectrum of a polypeptide is usually subdivided into three main regions of interest: 1) the range between 870 and 1150 cm^{-1} associated with the vibrations of the backbone Cα–C and Cα–N; 2) the range between 1230 and 1350 cm^{-1} containing the amide III region vibrations associated with normal modes of various combinations of the Cα–H and N–H deformations together with the Cα–C and Cα–N stretches [24]; 3) the range between 1630 and 1700 cm^{-1} associated with C=O stretching modes, defined amide I region [25].

In our case, the assignment of the primary structure features of Raman bands is very straightforward, since only Pro side-chains are present. For $(PPG)_{10}$ crystals, signals corresponding to the mother liquor (containing PEG 400 10%, sodium acetate 100 mM pH 5.3) are observed and are marked by a star in the Raman spectra. For $(PPG)_{10}$ powders, no background peak is expected. Frequencies corresponding to the major bands and their tentative assignments, proposed in agreement with previous studies [26], are reported in Table 1. The CH regions, reported in the supplementary material (Fig. S1), is similar to the proline spectrum [27].

Since crystals are isomorphous to those used for structural determination [1], the Raman crystallography study of $(PPG)_{10}$ provides the opportunity to define a relationship between vibrational properties and high-resolution structural details regarding both the φ and ψ torsional angles and the proline puckering.

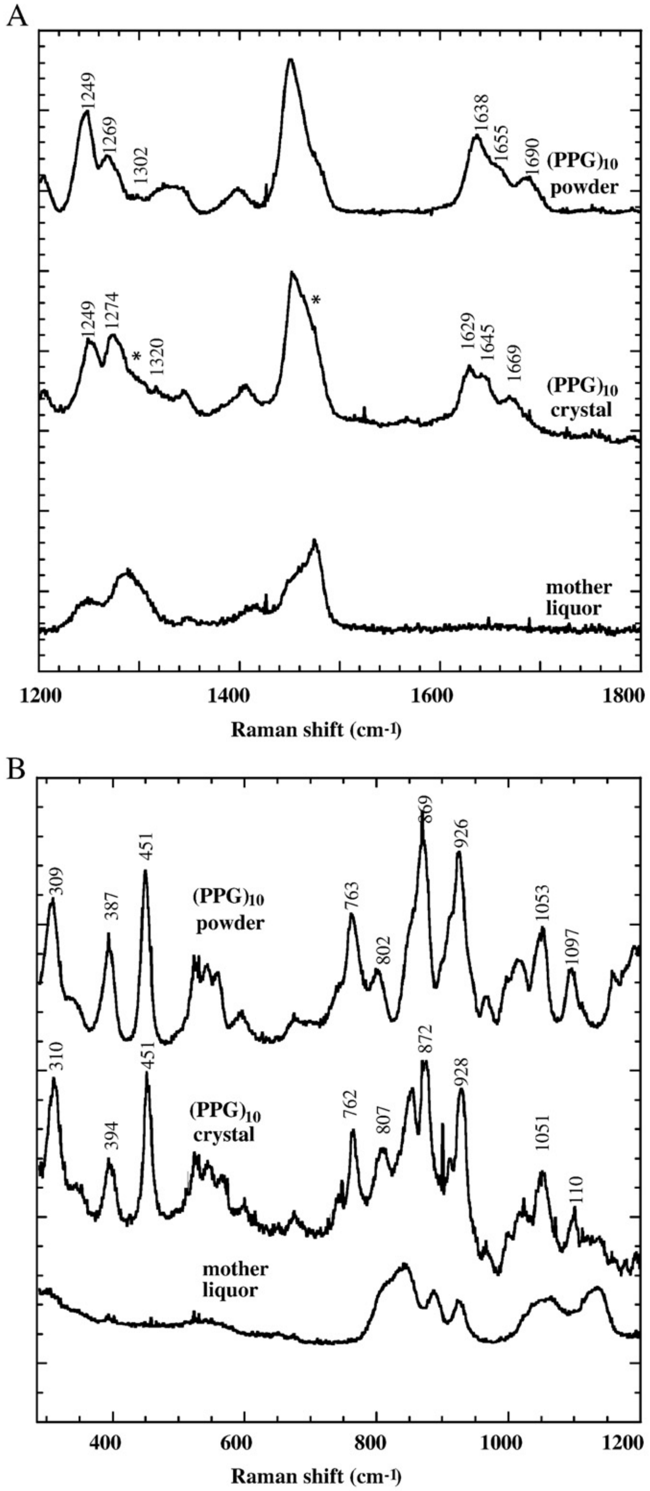

Fig. 1. Medium frequency (A) and low frequency (B) Raman spectra of $(PPG)_{10}$ powders, crystals, and mother liquor from which crystals grew up (ML). In spectra (A) and (B) the signals attributed to the mother liquor are tagged by a star. Spectral resolution is 4 cm^{-1}.

3.1. Amide bands

Raman amide I [28] and amide III [22] frequencies correlate with Ramachandran torsion angles and hydrogen bonds. Therefore, these

Table 1
Tentative assignment of the $(PPG)_{10}$ Raman shift

Band frequency (cm^{-1}) of $(PPG)_{10}$ crystal	Band frequency (cm^{-1}) of $(PPG)_{10}$ powder	Tentative assignment[a] of vibration modes
310 s	309	Delocalized modes
342 w	–	"
394 m	394	"
451 s	451	"
523 m	527	"
543 w	543	"
564 m	562	"
592 w	594	"
671 m	–	"
741 w	–	"
762 m	763	"
807 m	802	(C–C) stretch of backbone
854 m	–	(C–C) ring
872 s	869	–
911 w	–	Ring breathing modes
928 s	926	C–N, C–C stretch, CH bending, deloc
966 w	967	"
999 w	–	"
1013 w	1018	"
1022 w	–	"
1051 m	1053	"
1100 m	1097	"
1159 w	1160	"
1174 w	–	"
1194 w	1193	"
1205 w	1206	"
1249 s	1249	CH_2 rocking, amide III
1274 s	1269	"
1320 sh	1302	CH_2 wagging, amide III
1320	1329	CH_2 wagging
1343 w	–	CH_2 wagging
1452 vs	1398, 1452	Amide II, Cα–H bend, CH_2 scissoring
1629 s	1638	Amide I
1645 sh	1655	"
1669 m	1690	"

s: strong; m: medium; w: weak; sh: shoulder; vw: very weak.

[a] Assignment after Ref. [26]. A putative contribution of non-canonical amide III bands is also reported.

bands reveal secondary structure features and hydration level. The peculiar absence of intra/inter chain H-bond in the $(PPG)_{10}$ structure implies a relevant effect of the hydration patter to define the super-assembly [1,6]. The position of three amide I bands in $(PPG)_{10}$ crystals (1629, 1645 and 1669 cm^{-1}) is in good agreement with previous FT-IR absorption spectra of $(PPG)_{10}$ solution [29]. This finding provides strong evidence of similar hydration and Ramachandran angles between $(PPG)_{10}$ solutions and crystals, thus suggesting that crystal packing effects are not detectable for this $(PPG)_{10}$ Raman study. In the FT-IR study [29], the central peak has the highest absorbance, followed by the shoulders 1629 and 1667 cm^{-1}, whereas in this Raman study the 1629 cm^{-1} peak has highest intensity, followed by the peaks 1645 and 1669 cm^{-1}. These three bands correspond to three non-equivalent amide C=O groups in each of the Pro-Pro-Gly units. According to a previous study [29], the main peak at 1629 cm^{-1} comes mainly from the carbonyl of Pro in X position (with a small contribution of the glycyl group). The high frequency peak is mainly due to the carbonyl of Pro in Y position, whereas the central peak comes from the glycyl carbonyl, with a minor contribution of X and Y Pro carbonyls.

The amide I bands of $(PPG)_{10}$ crystals and powders are significantly different, not only for the intensity distribution of the crystal spectrum (depending on the orientation of the polarization of the exciting laser beam with respect to the main axes of the Raman tensor in the respective unit cell [30]), but also for the frequency of the Raman peaks. Analogously to $(PPG)_{10}$ crystals, spectra of $(PPG)_{10}$ powders are characterized by three distinct well-resolved amide I bands (1638, 1655, 1690 cm^{-1}), suggesting only one conformation (φ and ψ pair) for each residue of the repeating triplet. The three amide I bands, and especially the well-resolved band at 1690 cm^{-1}, do not match the frequencies reported by FT-IR solution studies for the unfolded $(PPG)_{10}$ (maximum at 1633 and a shoulder at 1665 cm^{-1}) or for the unfolded polyproline (one band at 1621 cm^{-1}) [29]. Therefore, the differences between amide I regions of $(PPG)_{10}$ powders and crystals might be attributed to a different hydration state, due to the lyophilization process used to prepare commercial powder.

The 1200–1350 cm^{-1} region of $(PPG)_{10}$, generalized as $(X\text{-}Y\text{-}G)_{10}$, is here reported for the first time. The analysis of the 1200 and 1350 cm^{-1} region is problematic for Pro residues. Indeed, prolines do not exhibit a canonical amide III vibration owing to the absence of a NH bond. Nevertheless, in this region two major bands can be distinguished, both for $(PPG)_{10}$ crystals and powders. For powders, two prominent bands are observed (1249 and 1269 cm^{-1}). Furthermore, a very minor higher frequency band has been observed at ca. 1302 cm^{-1}. For $(PPG)_{10}$ single crystals, two prominent shorter frequencies at ca. 1249 and 1274 cm^{-1} and a very minor higher frequency (ca. 1320 cm^{-1}) are observed.

The analysis of these three bands in the amide III (Table 1) has been tentatively carried out by a correlation between predicting equations derived for canonical amide III bands [21,22] and the structural information of $(PPG)_{10}$ average ψ angles previously reported [1]. In fact, though the φ angles vary as well along the helix [1], the φ angular dependence of amide III frequency is supposed to be small [22]. In general, predictive equations [21,22] capture the physics of the frequency dependence in that they calculate the ψ angular dependence of the coupling of the amide III vibration with Cα–H bending. If the 1200–1320 cm^{-1} region has a significant contribution of the non-canonical amide III bands expected for Pro residues, besides the CH_2 rocking–wagging bands, the comparison between experimental bands in the amide III region and predicted amide III frequencies is good for the Asher's equation [21] (see Table 2), but not for others [22]. Despite that the hydration, accurately described in the structural studies [1,6], is not included explicitly into the successful semi-empirical equation [21], the agreement between experimental and theoretical frequencies in the amide III region of $(PPG)_{10}$ is quite good. Within this assignment, the strong putative amide III bands correspond to the two proline residues in X and Y positions, whereas the very minor amide III bands correspond to the Gly amide bonds.

3.2. Proline puckering

Regarding the proline puckering in collagen-model peptides, multiple structural observations have been reported, as summarized in the Introduction section. Raman crystallography might shed light on this issue, since the preferential alternate *up* and *down* puckering of the proline ring observed in $(PPG)_{10}$ crystal structure [1] is expected to have a vibrational spectroscopy counterpart. Indeed, Raman bands are sensitive to the Pro ring puckering [26]. In particular, on the bases of DFT calculations performed on the two isomers (puckering *up* and *down*) of proline zwitterion, several vibrational modes are expected at different frequency, producing band broadening or even two well-resolved bands [26]. Though the two equally intense bands at 564 and 543 cm^{-1} in Fig. 1B might remind a doublet (568 and 546 cm^{-1}) for ring bending II (mode 7 in Ref. [26]) of the two *up* and *down* isomers reported by Kapitan et al. for Pro zwitterion [26], the inspection of

Table 2
Comparison between experimental data and predictions of the semi-empirical Asher's equation [21] [$\nu = 1265\ cm^{-1} - 46.8\ cm^{-1} \sin(\Psi + 5.2°)$] for the $(PPG)_{10}$ putative amide III bands

Peptidic bond	ψ_{exp} (°)	$AmIII_{exp}$ (cm^{-1})	$AmIII_{calc}$ (cm^{-1})
X-Y	164 ± 4	1274 ± 1	1272 ± 20
Y-G	152 ± 3	1249 ± 1	1259 ± 18
G-X	176 ± 3	1320 ± 1	1307 ± 15

(PPG)$_{10}$ crystal Raman spectra does not indicate other predicted doublets. This observation can be explained with a higher abundance of *down* Pro conformation in (PPG)$_{10}$ crystals [1,4,6] or with a failure in extending DFT calculations on Pro zwitterion and polyproline [26] to (PPG)$_{10}$. In the last case, further computational analyses are required to definitively assign the bands corresponding to the two *up* and *down* isomers of proline rings in (PPG)$_{10}$. Ultimately, this work does not support the indication of two distinct and equally populated up and down conformations of the pyrrolidine rings observed in the (PPG)$_{10}$ crystal structure.

Altogether these data suggest that Raman microscopy of single crystals is a valuable tool to study ring conformation and amide bands, detectable in solution only via UV Resonance Raman (UV-RR) spectra. Possible disadvantages of Raman crystallography versus UV-RR can be a) the presence of mother liquor and b) the risk of structural perturbation induced by packing contacts. On the other hand, advantages are a) a tight comparison between microscopic spectra and crystal structure, when compared under the same environmental conditions (e.g. temperature and cryoprotectant) and b) that UV-RR solution spectra register a distribution of aggregation states and of accessible torsional angles, possibly wider in solution than in the crystal phase.

Acknowledgment

This research was supported by Regione CAMPANIA (Legge 5).

Appendix A. Supplementary data

Supplementary data associated with this article can be found, in the online version, at doi:10.1016/j.bpc.2008.06.008.

References

[1] R. Berisio, L. Vitagliano, L. Mazzarella, A. Zagari, Crystal structure of the collagen triple helix model [(Pro-Pro-Gly)$_{10}$]$_3$, Protein Sci. 11 (2002) 262–270.

[2] S.K. Holmgren, L.E. Bretscher, K.M. Taylor, R.T. Raines, A hyperstable collagen mimic, Chem. Biol. 6 (1999) 63–70.

[3] L. Vitagliano, R. Berisio, L. Mazzarella, A. Zagari, Structural bases of collagen stabilization induced by proline hydroxylation, Biopolymers 58 (2001) 459–464.

[4] C. Hongo, K. Noguchi, K. Okuyama, Y. Tanaka, N. Nishino, Repetitive interactions observed in the crystal structure of a collagen-model peptide, [(Pro-Pro-Gly)$_9$]$_3$, J. Biochem. 138 (2005) 135–144.

[5] M.H. Li, P. Fan, B. Brodsky, J. Baum, Two-dimensional NMR assignments and conformation of (Pro-Hyp-Gly)$_{10}$ and a designed collagen triple-helical peptide, Biochemistry 32 (1993) 7377–7387.

[6] K. Okuyama, C. Hongo, R. Fukushima, G. Wu, H. Narita, K. Noguchi, Y. Tanaka, N. Nishino, Crystal structures of collagen model peptides with Pro-Hyp-Gly repeating sequence at 1.26 resolution: implications for proline ring puckering, Biopolymers 76 (2005) 367–377.

[7] M. Schumacher, K. Mizuno, H. Barchinger, The crystal structure of the collagen-like polypeptide (glycyl-4(*R*)-hydroxyprolyl-4(*R*)-hydroxyprolyl)$_9$ at 1.55 resolution shows up-puckering of the proline ring in the Xaa position, J. Biol. Chem. 280 (2005) 20397–20403.

[8] L. Tiansheng, C. Zhongguo, J.E. Johnson, G.J.J. Thomas, Structural studies of bean pod mottle virus, capsid, and RNA in crystal and solution states by laser Raman spectroscopy, Biochemistry 29 (1990) 508–5026 501.

[9] P.R. Carey, J. Dong, Following ligand binding and ligand reactions in proteins via Raman crystallography, Biochemistry 43 (2004) 8885–8893.

[10] A. Vergara, A. Merlino, E. Pizzo, G. D'Alessio, L. Mazzarella, A novel method for detection of seleno-methionine incorporation in protein crystals via Raman microscopy, Acta Cryst. D: Biol. Cryst. D64 (2008) 167–171.

[11] G.J.J. Thomas, Raman spectroscopy of protein and nucleic acid assemblies, Annu. Rev. Biophys. Biomol. Struct. 28 (1999) 1–27.

[12] G. Katona, P. Carpentier, V. Nivière, P. Amara, V. Adam, J. Ohana, N. Tsanov, D. Bourgeois, Raman-assisted crystallography reveals end-on peroxide intermediates in a non-heme iron enzyme, Science 316 (2007) 449–453.

[13] A. Merlino, C. Verde, G. di Prisco, L. Mazzarella, A. Vergara, Reduction of ferric hemoglobin from *Trematomus bernacchii* in a partial bis-histidyl state produces a deoxy coordination even when encapsulated into the crystal phase, Spectroscopy 22 (2008) 143–152.

[14] P. Carpentier, A. Royant, J. Ohana, D. Bourgeois, Advances in spectroscopic methods for biological crystals. 2. Raman spectroscopy, J. Appl. Cryst. 40 (2007) 1113–1122.

[15] R. Schweitzer-Stenner, F. Eker, A. Perez, K. Griebenow, X. Cao, L.A. Nafie, The structure of tri-proline in water probed by polarized Raman, Fourier Transform Infrared, vibrational circular dichroism, and electric ultraviolet circular dichroism spectroscopy, Biopolymers 71 (2003) 558–568.

[16] F. Eker, K. Griebenow, X. Cao, L. Nafie, R. Schweitzer-Stenner, Preferred peptide backbone conformations in the unfolded state revealed by the structure analysis of alanine-based (AXA) tripeptides in aqueous solution, Proc. Natl. Acad. Sci. US 101 (2004) 10054–10059.

[17] F. Eker, G. Griebenow, R. Schweitzer-Stenner, Ab1-28 fragment of the amyloid peptide predominantly adopts a polyproline II conformation in an acidic solution, Biochemistry 43 (2004) 6893–6898.

[18] B. Bochicchio, A.M. Tamburro, Polyproline II structure in proteins: identification by chiroptical spectroscopies, stability, and functions, Chirality 14 (2002) 782–792.

[19] A.V. Mikhonin, N.S. Myshakina, S.V. Bykov, S.A. Asher, UV Resonance Raman determination of polyproline II, extended 2.51-helix, and β-sheet ψ angle energy landscape in poly-L-lysine and poly-L-glutamic acid, J. Am. Chem. Soc. 127 (2005) 7712–7720.

[20] H. Torii, M. Tasumi, *Ab initio* molecular orbital study of the amide I vibrational interactions between the peptide groups in di- and tripeptides and considerations on the conformation of the extended helix, J. Raman Spectrosc. 29 (1998) 81–86.

[21] S.A. Asher, A.V. Mikhonin, S.V. Bykov, UV Raman demonstrates that α-helix polyalanine peptides melt to polyproline II conformations, J. Am. Chem. Soc. 126 (2004) 8433–8440.

[22] A.V. Mikhonin, S.V. Bykov, N.S. Myshakina, S.A. Asher, Peptide secondary structure folding reaction coordinate: correlation between UV Raman amide III frequency, ψ Ramachandran angle, and hydrogen bonding, J. Phys. Chem. B 110 (2006) 1928–1943.

[23] J. Garcia-Ruíz, L. Gonzalez-Ramirez, J. Gavira, F. Otálora, Granada Crystallisation Box: a new device for protein crystallisation by counter-diffusion techniques. Acta Cryst. D: Biol. Cryst. 58 (2002) 1638–1642.

[24] S.A. Asher, A. Ianoul, G. Mix, M.N. Boyden, A. Karnoup, M. Diem, R. Schweitzer-Stenner, Dihedral ψ angle dependence of the amide III vibration: a uniquely sensitive UV resonance Raman secondary structural probe, J. Am. Chem. Soc. 123 (2001) 11775–11781.

[25] S. Ngarize, H. Herman, A. Adams, N. Howell, Comparison of changes in the secondary structure of unheated, heated, and high-pressure-treated β-lactoglobulin and ovalbumin proteins using Fourier transform Raman spectroscopy and self-deconvolution, J. Agric. Food Chem. 52 (2004) 6470–6477.

[26] J. Kapitan, V. Baumruk, V. Kopecky, R. Pohl, P. Bour, Proline zwitterion dynamics in solution, glass, and crystalline state, J. Am. Chem. Soc. 128 (2006) 13451–13462; J. Kapitan, V. Baumruk, P. Bour, Demonstration of the ring conformation in polyproline by the Raman Optical Activity, J. Am. Chem. Soc. 128 (2006) 2438–2443.

[27] N.K. Howell, G. Arteaga, S. Nakai, E.C.Y. Li-Chan, Raman spectral analysis in the C–H stretching region of proteins and amino acids for investigation of hydrophobic interactions, J. Agric. Food Chem. 47 (1999) 924–933.

[28] M.M. Apetri, N.C. Maiti, M.G. Zagorski, P.R. Carey, V.E. Anderson, Secondary structure of α-synuclein oligomers: characterization by Raman and Atomic Force Microscopy, J. Mol. Biol. 355 (2006) 63–71.

[29] M. Bryan, J. Brauner, G. Anderle, C. Flach, B. Brodsky, R. Mendelsohn, FTIR studies of collagen model peptides: complementary experimental and simulation approaches to conformation and unfolding, J. Am. Chem. Soc. 129 (2007) 7877–7884.

[30] V. Pajcini, G. Chen, R. Bormett, S. Geib, P. Li, S. Asher, E. Lidiak, Glycylglycine π–π^* and charge transfer transition moment orientations: near-resonance Raman single-crystal measurements, J. Am. Chem. Soc. 118 (1996) 9716–9726.